Nanoscale Res Lett (2009) 4:187–190
DOI 10.1007/s11671-008-9215-4

NANO PERSPECTIVES

# Cu-Doping Effects in $CdI_2$ Nanocrystals: The Role of Cu-Agglomerates

**M. Idrish Miah**

Received: 12 September 2008 / Accepted: 11 November 2008 / Published online: 22 November 2008


**Abstract** Cu-doping effects in $CdI_2$ nanocrystals are studied experimentally. We use the photostimulated second harmonic generation (PSSHG) as a tool to investigate the effects. It is found that the PSSHG increases with increasing Cu content up to 0.6% and then decreases due to the formation of the Cu-agglomerates. The PSSHG for the crystal with Cu content higher than 1% reduces to that for the undoped $CdI_2$ crystal. The results suggest that a crucial role of the Cu-metallic agglomerates is involved in the processes as responsible for the observed effects.

**Keywords** Nanocrystals · Defects · Surface properties · Electron–phonon interaction

## Introduction

Nonlinear spectroscopy and photostimulated second harmonic generation (PSSHG) are the two important tools to investigate the higher-order nonlinear optical processes, in particular, in semiconductors [1]. The PSSHG is prevented by symmetry in a centrosymmetric material process. So, in order to observe the PSSHG, one needs to have a noncentrosymmetric process. Fortunately, there are different ways to enhance the PSSHG. These include (1) the reduction of the size of the crystals to the nanometer scale, (2) lowering the crystal temperature and (3) insertion of suitable impurities into the crystal with an appropriate amount [1]. The nanometer-sized crystals take into account the quantum-confined effect (quantum confinement dominates the material's electronic and optical properties), where **k**-space bulk-like dispersion disappears and discrete excitonic-like nanolevels occur within the forbidden energy gap.

$CdI_2$ single crystals are indirect and wide-bandgap semiconductors having layered structure, space group $C_{6v}^4$, with highly anisotropic chemical bonds. The band structure calculations of the $CdI_2$ crystals have also shown [2–4] a large anisotropy in the space charge density distribution causing high anisotropy in the corresponding optical spectra. The anisotropic behaviour of the $CdI_2$ crystals favours the local noncentrosymmetry, making them be able for the PSSHG investigations.

Experimental as well as theoretical investigations performed in pure $CdI_2$ single crystals in the last few years using nonlinear spectroscopy have shown that $CdI_2$ possesses higher-order optical nonlinearities [5–8]. An investigation for the magnetic field stimulated ferroelectricity in $CdI_2$–Cu has also been reported [9]. However, this measurement was preliminary performed a decade ago and the most recent report for this system is rare [10, 11].

Here we study Cu-doping effects in $CdI_2$ nanocrystals experimentally. We use the photostimulated second harmonic generation (PSSHG) as a tool to investigate the effects. It is found that the PSSHG increases with increasing Cu content up to 0.6% and then decreases due to the formation of the Cu-agglomerates, suggesting that a crucial role of the Cu-metallic agglomeration is involved in

M. I. Miah (✉)
Nanoscale Science and Technology Centre, Griffith University, Nathan, Brisbane, QLD 4111, Australia
e-mail: m.miah@griffith.edu.au

M. I. Miah
School of Biomolecular and Physical Sciences, Griffith University, Nathan, Brisbane, QLD 4111, Australia

M. I. Miah
Department of Physics, University of Chittagong, Chittagong 4331, Bangladesh

the processes. The PSSHG for the crystal with Cu content higher than 1% reduces to that for the undoped $CdI_2$ crystal.

## Experimental Details

Investigated samples are taken from 0.8 to 10 nm thick crystals of $CdI_2$ doped with Cu as well as undoped. Cu-doped $CdI_2$ nanocrystals were synthesized from the mixture of $CdI_2$ and CuI using standard Bridgman-Stockbarger method. Structure was monitored using an X-ray diffractometer and the homogeneity was controlled using a polarimeter. The nanocrystal sample thickness was controlled using a radio-frequency interferometer, using conventional fringe-shift technique as discussed in details in Ref. [12]. The investigation was performed at liquid nitrogen temperature by mounting the samples in temperature-regulated cryostat. We used a Nd:YAG laser, as a fundamental laser for the PISHG, which generates picosecond pulses (average power 15 MW) with a repetition rate of 80 mHz. The output PSSHG ($\lambda = 530$ nm) and fundamental ($\lambda = 1{,}060$ nm) signals were spectrally separated by a grating monochromator with a spectral resolution of $\sim 5$ nm mm$^{-1}$. Detection of the doubled-frequency (in the green spectral region) output PSSHG signal was performed by a photomultiplier (with time resolution about 0.5 ns), with an electronic boxcar integrator (EBI) for the registration of the output. During evaluation of the time-delayed nonlinear optical response, we measured the light intensities at the fundamental ($\omega$) and doubled-frequencies ($2\omega$) with time steps of $\sim 50$ fs using the EBI in the time-synchronized pump-probe conditions. The second-order effective susceptibilities were calculated using the relation [13]:

$$I(2\omega,t) = \frac{2\mu_0^{3/2}\varepsilon_0^{-3/2}\omega^2 l^2}{A}\frac{\chi_{ijk}^2 I^2(\omega, t-\tau)}{n(2\omega)n^2(\omega)}\left[\frac{\sin\frac{l\Delta k(t)}{2}}{\frac{l\Delta k(t)}{2}}\right]^2,$$

where $l$ is the length of the nonlinear medium, i.e. the crystal thickness, $\mu_0$ and $\varepsilon_0$ are the magnetic and dielectric static (in vacuum) susceptibilities, respectively, $A$ is the area of the pumping beam which processes Gaussian-like form, $n(\omega)$ and $n(2\omega)$ are, respectively, the refractive indices for the pumping and PSSHG doubled frequencies, $\chi_{ijk}$ are the components of the second-order nonlinear optical susceptibility determined from different angle of the incident light and $\Delta k = k(2\omega) - 2k(\omega)$ is phase matching wave vector factor defined by photostimulated birefringence. The light intensities of the time-dependent pumping $I(\omega,t)$ and frequency doubled PSSHG signals $I(2\omega,t-\tau)$ were measured for different times ($t$) of pulse duration and for different delaying times ($\tau$).

## Results and Discussion

The pumping power density dependence of the PSSHG signal was measured. Figure 1 shows the results for a crystal (0.8 nm). As can be seen, the PSSHG increases with increasing power density and then decreases to a value a little higher than background after reaching a maximum. The PSSHG dependence also shows a beginning of slight increase. However, a significant enhancement in PSSHG occurs for the nanocrystal. The qualitative and quantitative changes that occurred for the nanocrystal correspond to the manifestation of the quantum-confined excitonic levels perpendicular to the layer.

Figure 2 shows the pump-probe delay dependence of the PSSHG signal for a typical sample (1.2 nm; 0.8% Cu). As can be seen, the relaxation time of the signal is relatively large. Such a relaxation time is typically for the relaxation of a particular layer in layered crystals, where a significant contribution from the interlayer rigid phonons might be involved [14]. The relatively large relaxation time observed in the PSSHG pulses demonstrates the principal role of long-lived electron–phonon states in the observed effects explained within a model of photostimulated electron–phonon anharmonicity [15], where the relaxation time for the thin nanolayers should be larger than for the strong localized electron–phonon states due to the nanosized effects.

The second-order susceptibility determining the PSSHG as a function of sample thickness for a doped sample (0.8 %) is shown in Fig. 3. As can be seen, the PSSHG decreases with increasing the thickness of the crystal, and for the thickness higher than 10 nm, the PSSHG reduces to that for the undoped crystal (Fig. 4), demonstrating that a significant enhancement is achieved for the 0.8 nm thick crystal.

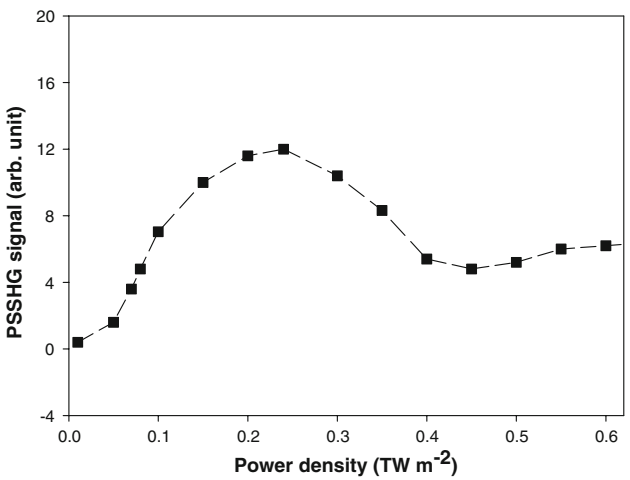


**Fig. 1** Pumping power density dependence of the PSSHG signal for a sample

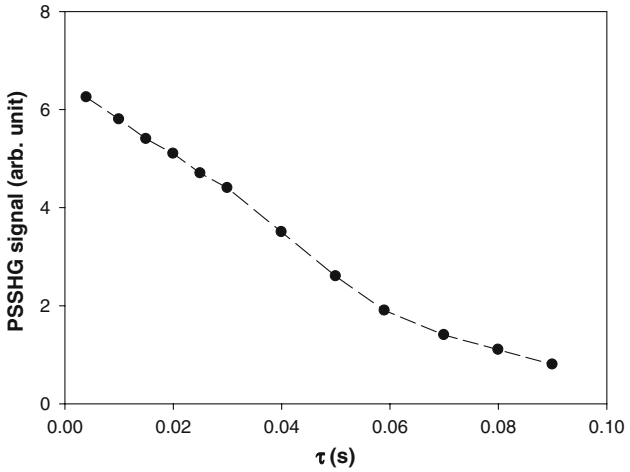


**Fig. 2** Pump-probe delay dependence of the PSSHG for a typical sample

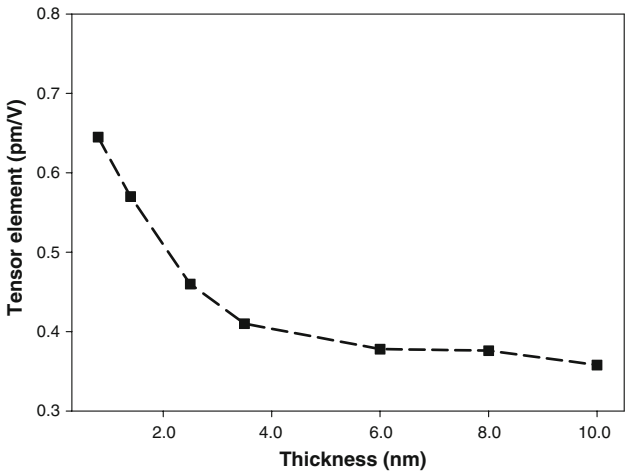


**Fig. 3** Second-order susceptibility as a function of sample thickness for a doped sample

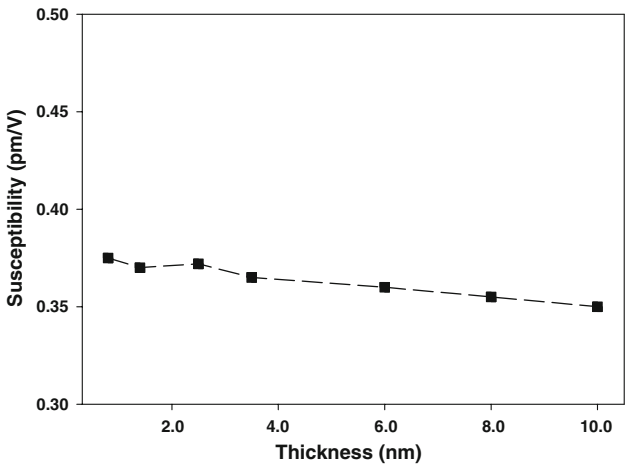


**Fig. 4** Second-order susceptibility as a function of sample thickness for the undoped sample

Figure 5 shows the second-order susceptibility as a function of Cu-doping density for a sample with crystal thickness 2.5 nm. The second-order susceptibility dependence of the Cu-doping density for a thin sample (0.8 nm) is shown in Fig. 6. From Figs. 5 and 6 one can see that with increasing Cu content up to 0.6% the PSSHG significantly increases. For the Cu content 0.6% the PSSHG achieves its maximum for a crystal with thickness 0.8 nm. The insertion of the Cu impurities favours a stronger local electron–phonon interaction, particularly its anharmonic part, through the alignment of the local anharmonic dipole moments by the pumping light [9]. As a particular role of the local electron–phonon anharmonicity is described by third-order rank tensors in disordered systems [10], the PSSHG is very similar to that introduced for the third-order nonlinear optical susceptibility, which has been confirmed by observing the relatively large third-order susceptibility of undoped $CdI_2$ single crystals [7]. The local disordering of the Cu agglomerates plays additional role in the nano-size-confined effects.

The PSSHG is found to be decreased for Cu density higher than 0.6%. This decrease of PSSHG with increasing Cu content is caused by agglomeration of the Cu impurities that is typical of such kinds of layered crystals. As demonstrated earlier [9], this can be understood in terms of the agglomerate chemistry. The creation of the Cu agglomerates favours a reduction in the active electron–phonon centres, effectively contributing to the noncentrosymmetry of the output charge density, as well as leads to the occurrence of metallic clusters which additionally scatter light, and consequently, suppresses the effect at higher Cu content through the limitation of the enhancement of the local hyperpolarizability for the Cu agglomerate as well as the corresponding nonlinear dielectric susceptibility. From the above analysis, one can conclude that a crucial role of

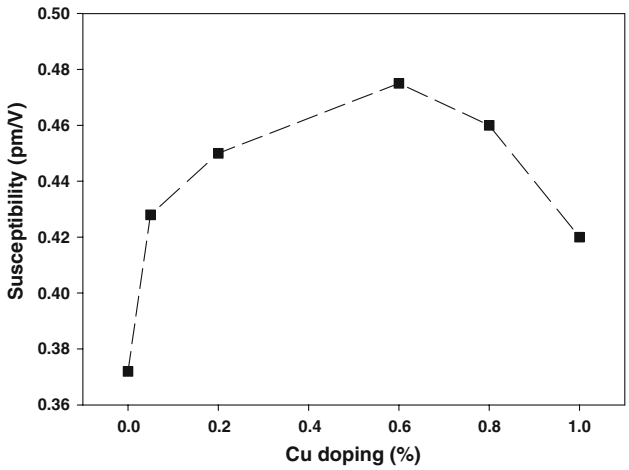


**Fig. 5** Second-order susceptibility as a function of Cu-doping density for a sample with thickness 2.5 nm

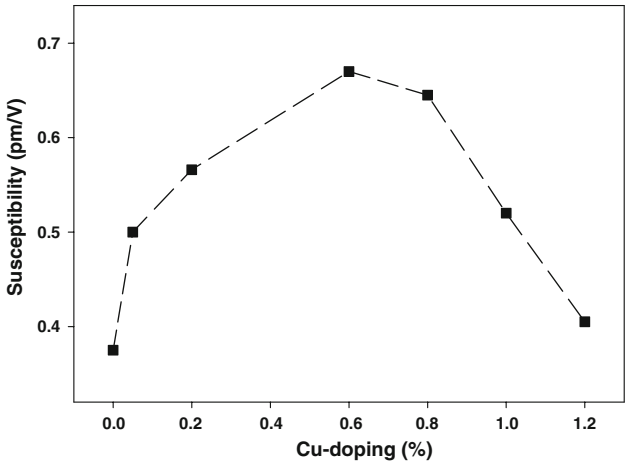


**Fig. 6** Second-order susceptibility as a function of Cu-doping density for a thin sample

the metallic agglomerates was involved in the processes and was responsible for the observed effects.

## Conclusions

Cu-doping effects in $CdI_2$ nanocrystals were studied experimentally using the PSSHG and the chemistry responsible for the effects discovered. It was found that the PSSHG increases with increasing Cu content up to 0.6% and then decreases due to the formation of the Cu-agglomerates, suggesting that a crucial role of the metallic agglomerates was involved in the processes. The PSSHG for the crystal with Cu content higher than 1% was found to be reduced to that for the undoped $CdI_2$ crystal.

## References

1. W.E. Born (ed.), *Ultrashort Processes in Condensed Matter* (Plenum Press, New York, 1993)
2. J. Bordas, J. Robertson, A. Jakobsson, J. Phys. C **11**, 2607 (1978)
3. J. Robertson, J. Phys. C **12**, 4753 (1979)
4. Ya.O. Dovgii, I.V. Kityk, Yu.M. Aleksandrov, V.N. Kolobanov, V.N. Machov, V.V. Michailin, J. Appl. Spectrosc. **43**, 1168 (1985). doi:10.1007/BF00662338
5. F. Adducci, I.M. Catalano, A. Cingolani, A. Minafra, Phys. Rev. B **15**, 926 (1977). doi:10.1103/PhysRevB.15.926
6. I.M. Catalano, A. Cingolani, R. Ferrara, M. Lepore, Helv. Phys. Acta **58**, 329 (1985)
7. M.I. Miah, Opt. Mater. **18**, 231 (2001). doi:10.1016/S0925-3467(01)00168-9
8. M.I. Miah, Opt. Mater. **25**, 353 (2004). doi:10.1016/j.optmat.2003.08.007
9. I.V. Kityk, S.A. Pyroha, T. Mydlarz, J. Kasperczyk, M. Czerwinski, Ferroelectrics **205**, 107 (1998). doi:10.1080/00150199808228391
10. V. Bondar, Mater. Sci. Eng. B **71**, 258 (2000). doi:10.1016/S0921-5107(99)00386-4
11. H. Ollafsson, F. Stenberg, Opt. Mater. **25**, 341 (2004). doi:10.1016/j.optmat.2003.08.010
12. I.V. Kityk, Z. Prikl, Spektrosck **42**, 487 (1985)
13. C.C. Devis, *Laser and Electro-Optics, Fundamentals and Engineering* (Cambridge University Press, New York, 1985)
14. S.A. Pyroha, S. Metry, I.D. Olekseyuk, I.V. Kityk, Funct. Mater. **7**, 209 (2000)
15. J.V. McCanny, R.H. Williams, R.B. Murray, P.C. Kemeny, J. Phys. C: Solid State Phys. **10**, 4255 (1977). doi:10.1088/0022-3719/10/21/014